Hindawi
Advances in Civil Engineering
Volume 2019, Article ID 9457309, 11 pages
https://doi.org/10.1155/2019/9457309

Research Article

Study on Relationship between UCS of Cemented Tailings Backfill and Weight Losses of Hydration Products

Bingwen Wang,[1] Lijing Gao ,[1] Tingyong Xiong,[1] Xiangyu Cui,[1] Yanan Li,[2,3] and Kai Lei[1]

[1]*School of Energy & Mining Engineering, China University of Mining & Technology (Beijing), Beijing 100083, China*
[2]*Zijin Mining Group Co., Ltd., Longyan, Fujian 364200, China*
[3]*Shanxi Zijin Mining Co., Ltd., Xinzhou, Shanxi 034300, China*

Correspondence should be addressed to Lijing Gao; 1035506605@qq.com

Received 29 June 2019; Accepted 3 September 2019; Published 18 September 2019

Academic Editor: José Aguiar

The weight losses of cement-based material samples were often used to characterize the content of their hydration products and explain the strength changes of cement-based materials. However, the quantitative relationship has not been studied between the weight loss of hydration products and strength of cement-based materials. This paper studied the relationship between the strengths of cemented tailings backfills (CTBs) and the weight losses of its hydration products. The CTB samples have been done, especially on different binders, cement-tailing ratios, mass concentrations, and different curing ages. The uniaxial compressive strength (UCS) experiments were used to test the mechanical strength of samples; X-ray diffraction (XRD) experiments were used to test the crystalline phases of hydration products by samples; thermal analyses (thermogravimetric and differential thermogravimetric (TG/DTG)) experiments were used to test the weight losses of hydration products. By means of regression analysis, the relationship model was established between the UCS of CTB and the weight losses of hydration products at different concentrations. The results show that there is a strong linear correlation between the UCS and the weight loss of the hydration product calcium silicate hydrate (C-S-H) for the CTB made of glue powder, while the UCS is related to the weight losses of C-S-H and $Ca(OH)_2$ for the CTB made of ordinary Portland cement. The results acquired by this paper provide a scientific basis for studying hydration products by thermal analyses and explaining the strength changes of cement-based materials.

1. Introduction

During the consolidation process of the cemented tailings backfill (CTB), ettringite (Aft), hydrated calcium silicate (C-S-H), calcium hydroxide, and other hydration products will be produced [1–4]. The strength of backfill is closely related to the content of these hydration products [5, 6]. Thermal analyses (thermogravimetric and differential thermogravimetric (TG/DTG)) are often used to study the hydration products of cement-based materials, and the weight losses of the hydration products are obtained by TG-DTG experiments [7–11].

Many scholars have used the weight losses of the hydrated products to characterize the relative or absolute content of the hydrated product, thereby explaining the change of the strength of the cement-based material. Fall studied the relationship between the strength of the backfill and the hydration products. It was found by thermal analyses that endothermic peaks and weight losses in the 50~150°C, 450°C, and 750°C temperature ranges are higher for the PCI (backfill made of Portland cement type I) specimens than for the FA (backfill made of fly ash), so it is considered that the content of C-S-H, AFt, $Ca(OH)_2$, and $CaCO_3$ formed with PCI is higher than FA, and the strength of PCI specimens is higher [12]. Jiang et al. analyzed the TG/DTG curve of CPB (cemented paste backfill) at different curing temperatures. A comparison of the TG/DTG diagrams for the CPBs shown that the first and second peaks or changes in weight were much higher for CPB cured at 23.5°C, and it indicated that more hydration products (e.g., calcium hydroxide and C–S–H) are formed in CPB, so its yield stress was higher [13]. Kun and Fall studied the TG/DTG curve of CPB samples under different curing conditions. It was found that their weight loss (at temperatures

between 110°C and 200°C) of the sample cured at 35°C is greater than the sample cured at 20°C. And the sample cured at 35°C is considered to produce more hydration products in the CPB sample [14]. Wang et al. researched the TG curve of slag-fly ash composite cement. It is believed that the C-S-H and C-A-H (calcium hydrated calcium aluminate) dehydrates when heated to 100~400°C, and $Ca(OH)_2$ is decomposed when heated to 400~500°C. The amount of hydration product was analyzed by the weight loss at the two temperature ranges [15]. Hou et al. carried out TG/DTG experiments on a new cementitious material (NCM) and ordinary Portland cement (OPC) samples. It indicated that the weight loss of the NCM sample at 110~200°C is more than OPC. And it is believed that more cement-based hydration products were generated in the NCM, so the stress of the NCM sample is higher [16]. Ding quantitatively analyzed the hydration products of concrete materials by means of thermal analyses [17].

According to the above studies, we found that two main disadvantages exist in these studies. On the one hand, the thermal decomposition temperature of AFt is similar to C-S-H gels. If no special treatment is applied to the samples, two weight loss peaks often coincide [18, 19]. Hence, the weight loss before 200°C is only considered to be the weight loss peak of one of AFt or C-S-H gels is unreasonable. On the other hand, it is not reasonable that calculating the C-S-H gel content by weight loss of C-S-H gel. Furthermore, it is also unsuitable for explaining the strength change. Because the hydration product C-S-H gel is amorphous and its chemical composition is not fixed, it is difficult to quantitatively analyze C-S-H gel according to its weight loss. At present, it is difficult to quantitatively determine the content of hydration products, especially the C-S-H gel cannot be determined by thermal analyses, but the relationship can be directly studied between the strength and weight loss of hydration products by means of statistical methods.

Therefore, this paper focuses on the relationship between the uniaxial compressive strength (UCS) of the CTB and the weight losses of the hydration products. The UCS values and the weight losses of the hydration products were obtained by the UCS tests and thermal analyses (TG/DTG). The relationship between the weight losses of hydration products and UCS of CTB was established by the regression analysis. The results of this study provide a scientific basis for studying hydration products by thermal analyses and explaining the strength changes of cement-based materials.

2. Materials and Methods

2.1. Materials. The materials consist of water, OPC 42.5# (Jilong Cement Co., Ltd., Tangshan, China), glue powder (a binder used in the Linglong Gold Mine filling station, Linglong Gold Mining Co., Ltd., Zhaoyuan, China), and tailings (Linglong Gold Mining Co., Ltd., Zhaoyuan, China).

2.1.1. Water and Binder. The water used for the experiment is tap water. Glue powder (GP) is a binder used in the Linglong Gold Mine filling site, and the main components of GP are slag and cement clinker. OPC was the most familiar binder used in the disposing of the tailings [20]. The performance results of the GP to CTB were compared with that of OPC. The main chemical constituents of the GP and OPC are shown in Table 1.

2.1.2. Tailings. The tailings were full tailings taken back from the site. The full tailings were dried. The particle size characteristics were analyzed, and the result is shown in Table 2. The d_{10}, d_{30}, d_{50}, d_{60}, and d_{90} represent the cumulative content of the particle composition curve, with a corresponding particle size of (volume fraction) 10%, 30%, 50%, 60%, and 90%, respectively. The median particle size was 101.74 μm, which is characteristic of fine tailings. The main chemical composition of the tailings is shown in Table 3.

2.1.3. Preparation of CTB Samples. The CTB is composed of tailings, binder, and water. CTB samples with different binders (GP and OPC), mass concentrations (65%, 68%, 70%, 72%, 75%, and 78%) and cement-tailing ratios (1 : 4, 1 : 6, 1 : 8, and 1 : 10) were prepared. The required amounts of tailings, binder, and water are mixed and homogenized in a mixer until obtaining the desired mixtures. Afterwards, the produced cemented tailings backfill mixtures are poured into curing cubes (7.07 cm × 7.07 cm × 7.07 cm) to form cubic CTB samples. Three identical samples were prepared for each CTB. The GP paste with a mass concentration of 65% was prepared, and the paste was poured into a cubic mold (20 mm × 20 mm × 20 mm). Then, these samples are cured in a YH-40B standard curing chamber at a temperature of 20 ± 1°C for period of 7, 14, and 28 days.

For convenience of description, "G04-65-7" is used to indicate the CTB sample with GP as a binder, cement-tailings ratio of 1 : 4, mass concentration of 65%, and curing age of 7 days. "P08-72-14" is used to indicate the CTB sample with OPC as a binder, cement-tailings ratio of 1 : 8, mass concentration of 72%, curing age of 14 days, and so on ("G" means the CTB samples with GP as binder, and "*P*" means the CTB samples with OPC as binder).

After the CTB samples were cured to the specified time, the UCS test was performed, and the test results were taken as the average of the UCSs of the three identical CTB samples. The GP paste samples were crushed and sampled after 3 d, 7 d, and 28 d, respectively. The samples of the central part of CTB and GP paste were taken and treated with ethanol to terminate the hydration [21]. Then, they were dried in an oven at 80°C to a constant weight to remove ettringite in the sample [22]. Finally, the samples were ground into powder. And XRD and thermal analysis test samples were obtained.

2.2. Experimental Methods

2.2.1. The UCS Experiment. The mechanical strength or the stability of the CTB samples was usually evaluated using UCS [20, 23, 24]. UCS tests were carried out on the different

Table 1: Main chemical constituents of the materials.

Element unit	SiO_2 (wt.%)	Al_2O_3 (wt.%)	K_2O (wt.%)	Na_2O (wt.%)	CaO (wt.%)	Fe_3O_4 (wt.%)	MgO (wt.%)	S (wt.%)
GP	20.40	9.33	0.59	0.28	53.08	1.27	4.51	3.21
OPC	21.86	15.49	0.34	0.35	63.59	2.66	2.19	2.42

Table 2: Particle size characteristics of tailings.

Element unit	d_{10} (μm)	d_{30} (μm)	d_{50} (μm)	d_{60} (μm)	d_{90} (μm)	Cc	Cu
Tailings	8.51	37.81	101.74	134.73	245.59	15.83	1.25

Table 3: Main chemical constituents of the tailings.

Element unit	SiO_2 (wt.%)	Al_2O_3 (wt.%)	K_2O (wt.%)	Na_2O (wt.%)	CaO (wt.%)	Fe_3O_4 (wt.%)	MgO (wt.%)	S (wt.%)
Tailings	66.90	18.06	4.70	2.85	2.27	1.52	0.88	0.25

CTB samples in accordance with TYE-300D (Wuxi Jianyi Instrument Machinery Co., Ltd., Wuxi, China). The load was executed at rate 0.01 kN/s. The test process is shown in Figure 1.

2.2.2. The XRD Experiment. XRD was a common measurement for crystal phase structure identification in cement-based materials slurry [25]. XRD was performed on the prepared samples using a SmartLab high-resolution X-ray diffractometer (initial setting: starting angle 5°, ending angle 90°, step size 0.02°, scanning speed 15°/min, and anode material Cu target), as illustrated in Figure 2. Test analysis was carried out to determine the crystalline phases of hydration products and CTBs.

2.2.3. The TG/DTG Experiment. TG and DTG tests were performed on different CTB samples to determine the weight losses of various hydration products of the samples. This was done using a STA449F3 TG analyzer (NET Scientific Instruments Trading (Shanghai) Co., Ltd., Shanghai, China) that can raise temperatures up to 1550°C, as illustrated in Figure 3. The temperature was increased from room temperature to 1200°C at a rate of 10°C/min N_2 purge. The reason why the temperature not raised to 1550°C was that the mass quality does not change when the temperature was higher than 1200°C.

3. Results and Discussion

3.1. UCS of the CTB. Factors affecting the physical and mechanical properties of the CTB include the type of binder, the ratio of cement to tailing, the mass concentration of the slurry, the age of the curing, particle gradation of tailings, etc. [4]. The tailings used in the test are full tailings, which are characterized by fine particles, unreasonable gradation, and high mud content. Using of OPC as binder, there are problems such as high cost and low consolidation strength. The uniaxial compressive strength test results of OPC-CTB and GP-CTB are shown in Figure 4. For convenience of expression, "G04" in the figure is the CTB sample with GP as binder, cement-tailings ratio 1 : 4. "P08" is the CTB sample with OPC as binder, cement-tailings ratio 1 : 8, and so on.

Figure 4 clearly shows that the strength of GP-CTB is greater than that of OPC-CTB under the same conditions, especially early strength. The GP is a better binder for full tailings, and the GP-CTB has the characteristics of quickly hardens and high strength. For full tailings, GP performance is superior to OPC. In addition, it can be seen from Figure 4 that the strength of CTB is directly related to the cement-tailings ratio and curing age. The more binder is added, the higher the mechanical strength of the CTB. And the UCS will increase with the curing age increasing. The influence of cement-tailings ratio and curing age on UCS is easy to understand. As the amount of binder or curing age increases, more hydration products will be produced in CTB.

3.2. The Crystalline Phases of Hydration Products. XRD experiments were performed on prepared GP paste and GP-CTB samples to test the crystalline phases of hydration products. Figure 5 shows the XRD patterns of GP pastes with a mass concentration of 65% at different curing ages. It can be seen from Figure 5 that the amorphous C-S-H gels are contained in the GP paste of different curing ages. The peaks shape of C-S-H is dispersed, and the main characteristic peak is 0.307 nm (29.5°). As the curing age increases, the relative intensity of the main characteristic peak of C-S-H gel increases, indicating that the C-S-H gel content increases. However, there were a large number of diffuse peaks in the samples with the curing age of 28 d, indicating that the crystallinity of the C-S-H gel did not increase significantly with the increase of the curing age, which was consistent with the description in the literature [26, 27]. In addition, the samples also contain a certain amount of ettringite, which indicates that a small amount of ettringite has not been decomposed after the samples are dried at 80°C.

By performing XRD experiments on the CTB samples, the phase composition of the CTB samples is directly obtained. Figure 6 shows the XRD patterns of the G04-65-7, G04-65-14, and G04-65-28 samples. It can be seen from Figure 6 that the CTB samples mainly contain mineral components such as quartz, feldspar, calcite, and muscovite.

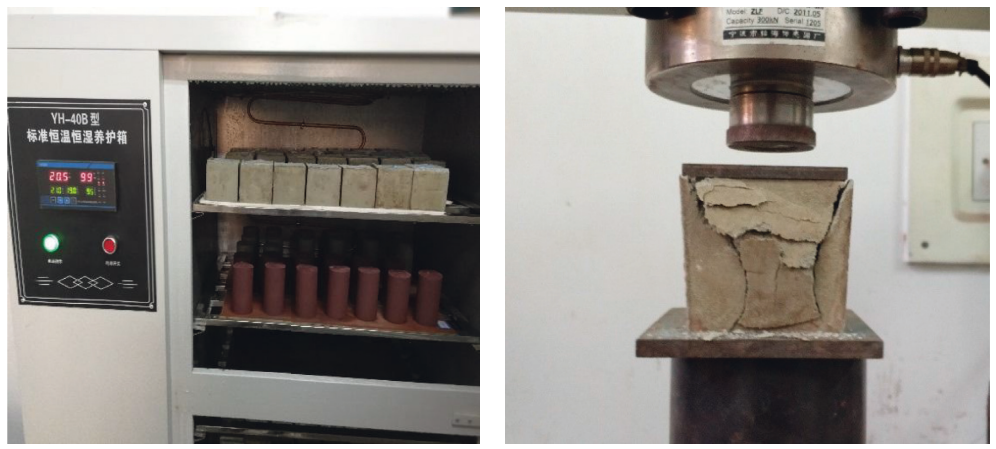

(a) (b)

Figure 1: Uniaxial compressive strength test process. (a) The CTB samples; (b) the TYE-300D and the destroyed CTB sample.

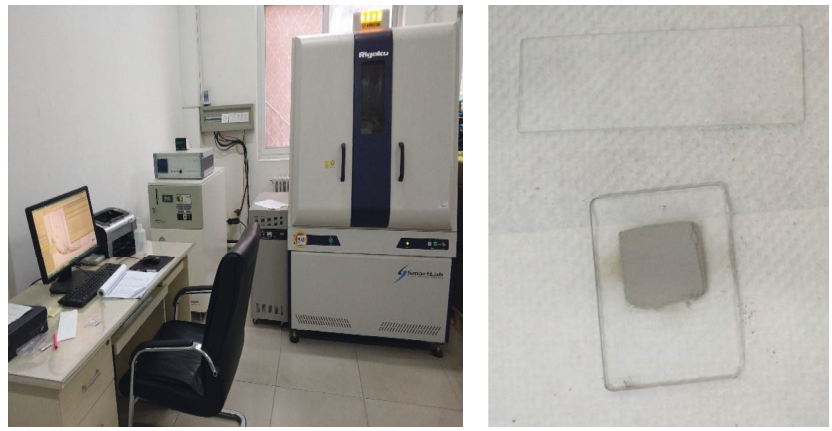

(a) (b)

Figure 2: The Empyrean Diffractometer and sample. (a) The X-ray diffraction (XRD) analyzer; (b) the sample.

(a) (b)

Figure 3: STA449F3 and sample carrier. (a) STA449F3 thermal analyzer; (b) sample carrier.

Among the hydration products, only the C-S-H diffraction peak was obvious, and ettringite was not observed. It can be explained due to the following three reasons: Firstly, most of the components in the CTB sample are tailings. Secondly, in the hydration products of the GP, the C-S-H content is the majority, and the ettringite content is relatively small [26]. Thirdly, the ettringite has been decomposed after drying at 80°C.

Previous works have been studied the phase composition of the OPC hydration products [16, 22, 28, 29]. The

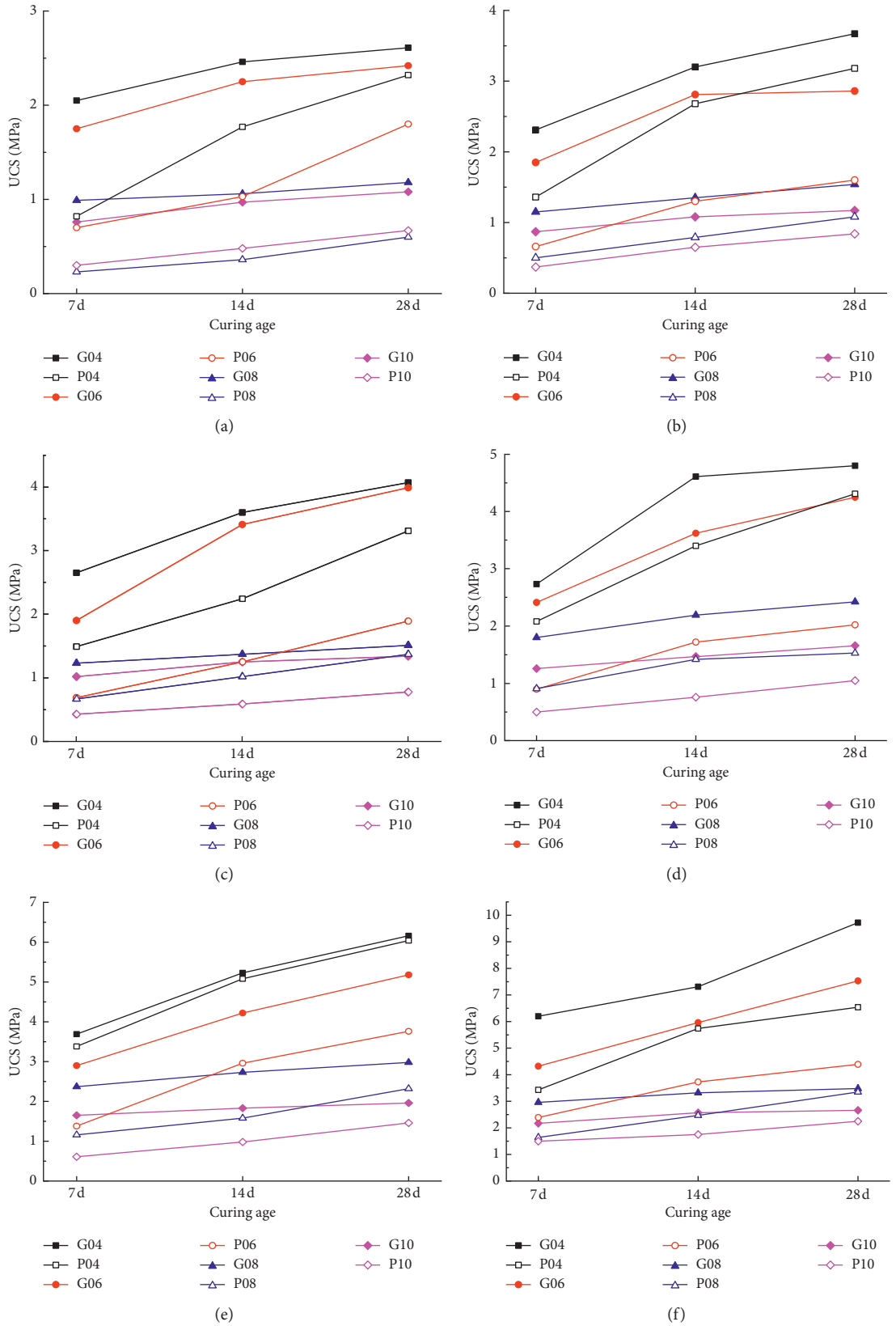

Figure 4: Diagram of CTB strength growth: (a) mass concentration 65%; (b) mass concentration 68%; (c) mass concentration 70%; (d) mass concentration 72%; (e) mass concentration 75%; (f) mass concentration 78%.

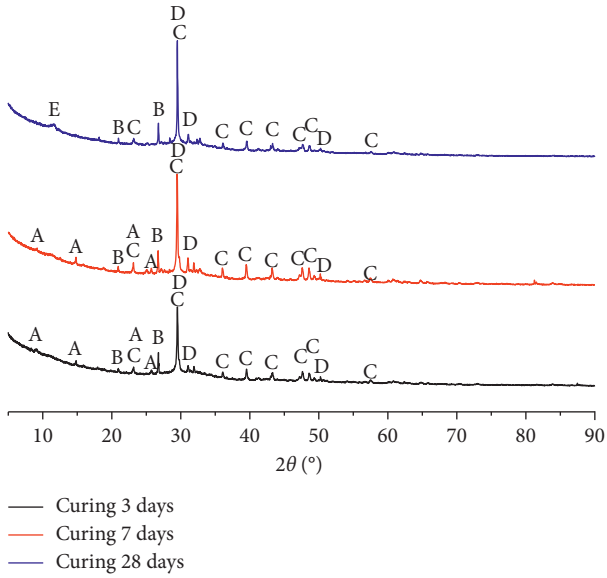

Figure 5: X-ray diffraction pattern of GP pastes with a mass concentration of 65% for curing 3 d, 7 d, and 28 d. (A) Ettringite; (B) feldspar; (C) calcite; (D) C-S-H gel; (E) tetracalcium aluminate hydrate.

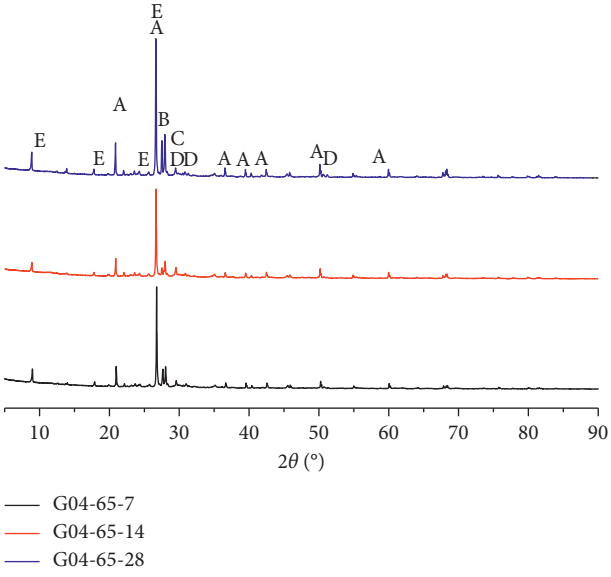

Figure 6: X-ray diffraction pattern of GP-CTB samples. (A) Quartz; (B) feldspar; (C) calcite; (D) C-S-H gel; (E) muscovite.

hydration products include C-S-H, $Ca(OH)_2$, and $CaCO_3$. Therefore, XRD analysis is not carried out for samples of the OPC-CTB and OPC paste.

3.3. Weight Losses of Hydration Products

3.3.1. The Weight Losses of Hydration Products of GP-CTB. TG/DTG experiments were performed on prepared GP paste and GP-CTB samples to test the weight losses of the hydration products. Figure 7 shows the TG/DTG diagram of GP pastes for curing 28 days. As can be seen from Figure 7,

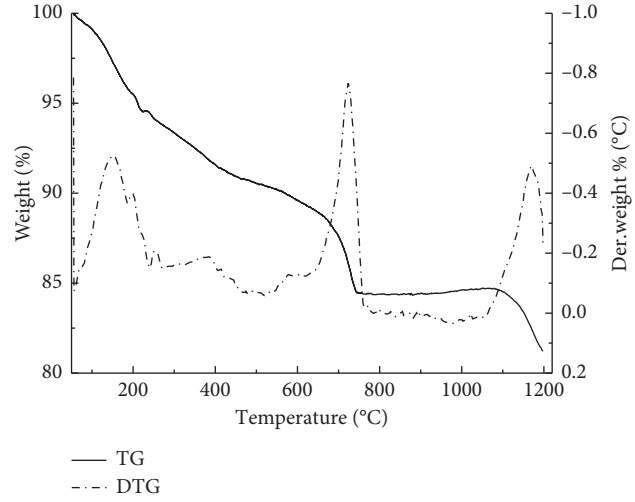

Figure 7: TG/DTA diagram of GP paste for curing 28 days.

there are three weight loss peaks in the sample. The first peak (DTG) or change in weight (TG) is found between 100°C and 200°C, resultant of the dehydration reactions of the C-S-H [22, 30, 31]. The C-S-H gel is mainly derived from the hydration reaction of clinker minerals:

$$3CaO \cdot SiO_2 + nH_2O \longrightarrow xCaO \cdot SiO_2 \cdot yH_2O + (3 - x)Ca(OH)_2 \quad (1)$$

$$2CaO \cdot SiO_2 + mH_2O \longrightarrow xCaO \cdot SiO_2 \cdot yH_2O + (2 - x)Ca(OH)_2 \quad (2)$$

The ratio of silicon to calcium (S/C) and water to silicon (H/S) of C-S-H is not constant, which varies with a series of factors [26]. Therefore, the C-S-H content cannot be accurately measured based on the weight losses of it. The occurrence of the second peak or change in weight, which is observed at 650~750°C, is mainly due to the decomposition of the calcite [32, 33]. The $CaCO_3$ in the sample is mainly derived from the carbonization of hydration products. The essence of carbonization is that carbon dioxide enters the interior of the sample and dissolves in the water of the internal pore surface to form carbonic acid, which neutralizes the alkaline matter in the hydration product. The hydration reaction of the GP first generates $Ca(OH)_2$, and then reacts with CO_2 in the air to form $CaCO_3$ [34]. Finally, the third peak or change in weight is found between 1100°C and 1200°C, and it was attributed to the decomposition of some unknown hydration product. There is no research report on this kind of hydration product, but the relationship between the weight loss at this peak and the strength of the CTB can still be studied.

TG/DTG experiment is carried out on the CTB samples to obtain the weight losses of the hydrated products of CTB, so as to construct a relationship model between the UCS of the CTB and the weight losses of the hydrated products. Taking G04-70-28 as an example, the TG/DTG diagram of it is shown in Figure 8. The weight loss process of the other GP-CTB samples is similar to that of G04-70-28. According

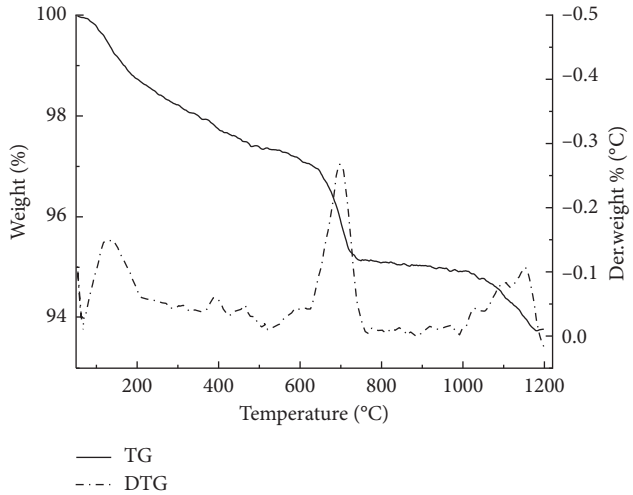

Figure 8: TG/DTA diagram of G04-70-28.

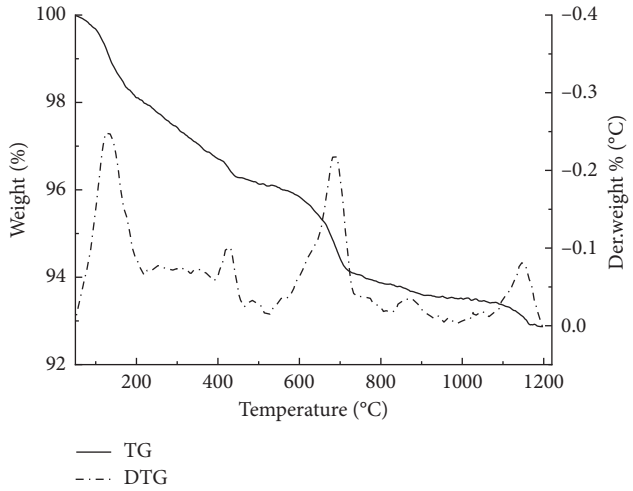

Figure 9: TG/DTA diagram of P04-70-28.

to the three weight loss peaks of the DTG curve, the TG curve of the sample is divided into three weight loss stages. In the first stage, the peak temperature of weight loss is 137.22°C, and the weight loss is 1.45%, corresponding to the dehydration reactions of the C-S-H. In the second stage, the peak temperature of weight loss is 687.23°C, and the weight loss is 1.90%, corresponding to the thermal decomposition of $CaCO_3$. In the third stage, the peak temperature of the weight loss is 1129.44°C, and the weight loss is 1.16%, attributed to the decomposition of the unknown hydration product.

3.3.2. The Weight Losses of Hydration Products of OPC-CTB. TG/DTG experiments were performed on prepared OPC-CTB samples to test the weight losses of the hydration products. For OPC paste, a scholar conducted a thermal analyses experiment and found that its hydration products include C-S-H, $Ca(OH)_2$, and $CaCO_3$ [16]. Therefore, the TG/DTG curve of OPC paste is not listed in this paper.

Taking P04-70-28 as an example, the TG/DTG diagram of it is shown in Figure 9. The weight loss process of the other OPC-CTB samples are similar to that of P04-70-28. As can be seen from the DTG curve in Figure 9, the sample has four weight losses in the TG/DTG experiment. In the first stage, the peak temperature of weight loss is 128.51°C, and the weight loss is 1.90%, corresponding to the dehydration reactions of the C-S-H. In the second stage, the peak temperature of weight loss is 422.34°C, and the weight loss is 0.44%, attributing to the de-hydroxylation of $Ca(OH)_2$ [16, 32, 33, 35]. In the third stage, the peak temperature of weight loss is 689.10°C, and the weight loss is 1.86%, corresponding to the thermal decomposition of $CaCO_3$. In the fourth stage, the peak temperature of the weight loss is 1155.31°C, and the weight loss is 0.55%. And the weight loss stage is similar to the third weight loss stage of the GP-CTB, attributed to the decomposition of the unknown hydration product. Compared with the TG/DTG curve of GP-CTB samples, there is a weight loss peak of $Ca(OH)_2$ in the OPC-CTB samples. This indicates that OPC hydration produces $Ca(OH)_2$, while $Ca(OH)_2$ is scarcely present in the GP hydration product.

3.4. Relationship between Strength of CTB and Weight Loss of Single Hydration Product. The CTB samples were divided into 12 groups according to the concentration and the binder used, and the relationship was studied between the weight loss of hydration products and the UCS of CTB. (The reason for classifying CTB according to the concentration and binder is that only when concentration and binder are same, the hydration product content is the only factor affecting the strength of CTB).

The TG curves of the GP-CTBs were divided into three weight loss stages, so linear regression fitting was performed on the UCS with weight losses of hydration products in three stages respectively. The results are shown in Figure 10, where R^2 is the correlation coefficient. It can be seen from Figure 10 that the weight loss of hydration products C-S-H gel has a positive correlation with its UCS, while the weight loss of $CaCO_3$ and weight loss in the third stage have a little or no correlation with the UCS. This indicates that the C-S-H gel has the greatest contribution to the UCS of GP-CTB.

The TG curves of the OPC-CTB samples are divided into four weight loss stages, so linear regression fitting was performed on UCS with weight losses of hydration products in four stages respectively. The results are shown in Figure 11. It can be seen from Figure 11 that the weight loss of hydration products C-S-H gel and $Ca(OH)_2$ have a positive correlation with its UCS, while the weight loss of $CaCO_3$ and weight loss in the fourth stage have a little or no correlation with UCS. This indicates that the C-S-H gel and $Ca(OH)_2$ of the OPC hydration product are important factors influencing the UCS of the OPC-CTB.

3.5. Relationship Model of Strength and Weight Losses of Hydration Products. Since the UCS of OPC-CTB is related to the weight losses of hydration products C-S-H and $Ca(OH)_2$, multiple regression analysis is performed on the UCS with weight loss of C-S-H gel and $Ca(OH)_2$. The

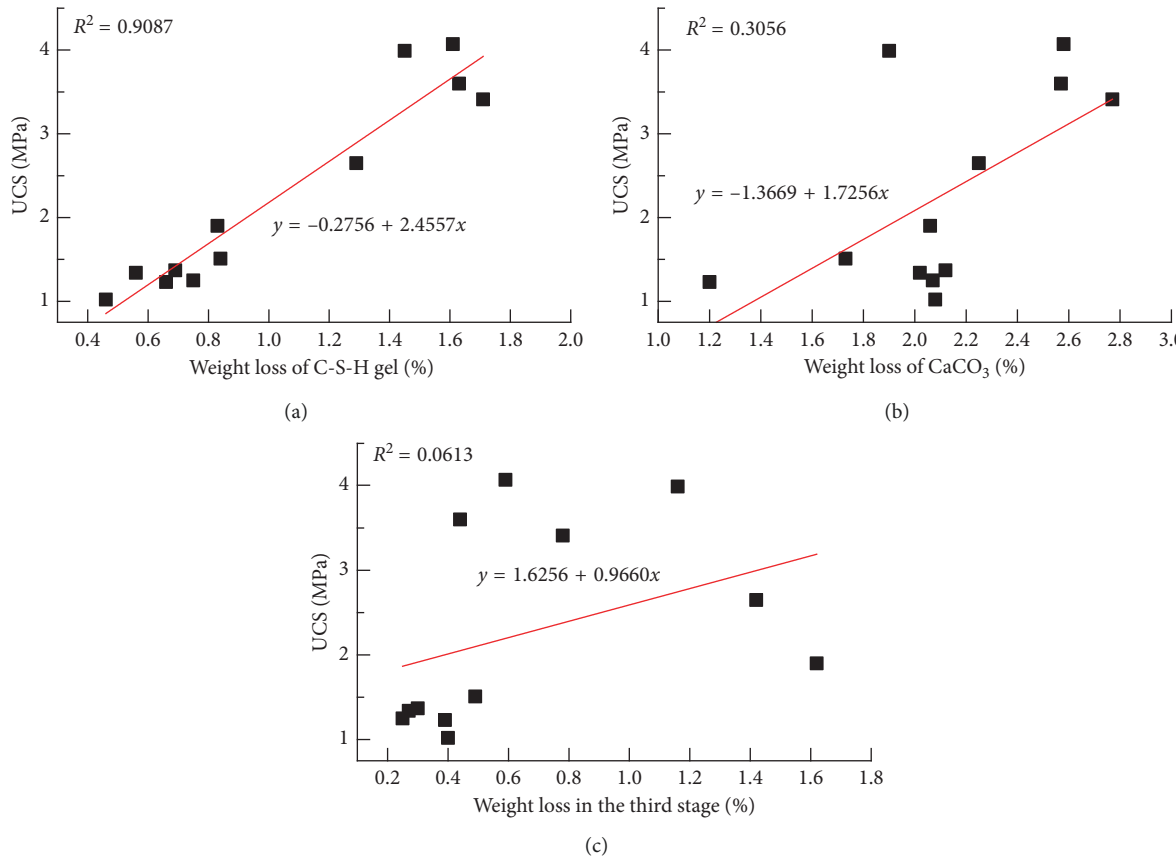

Figure 10: Fitting diagrams of weight loss of hydration products and UCS of GP-CTB (mass concentration 70%). (a) Fitting diagram of weight loss of C-S-H gel and UCS of GP-CTB; (b) fitting diagram of weight loss of $CaCO_3$ and UCS of GP-CTB; (c) fitting diagram of weight loss in third stage and UCS of GP-CTB.

relationship model between the UCS of the CTB and the weight losses of the hydrated products is established as shown in Table 4. For the OPC-CTB, the R^2 of the binary linear regression equation increases and the regression effect is more significant than the linear regression equation. From the Table 4, the quantitative relationship between UCS of CTB and weight loss of the hydration product can be clearly seen. For GP-CTB, UCS depends linearly on weight loss of C-S-H, while for OPC-CTB, both weight losses of C-S-H and $Ca(OH)_2$ on the UCS have significant effects on UCS. CTB with larger weight losses of the hydration products has a higher UCS. The correlation coefficients of all equations are greater than 0.7, indicating that the established relationship model is reliable.

4. Conclusions and Future Work

Two kinds of CTB samples were made by OPC and GP, respectively. The UCS of the CTB samples was measured by the uniaxial compressive strength test. The phase of hydration products was determined by XRD experiment. The weight loss of the sample hydration product was determined by TG/DTG experiment. The relationship model between the UCS of the CTB and the weight losses of the hydrated products was established in this paper. The major findings of this study included the following:

(1) Compared with OPC, the GP is a better cementing material for full tailings, and the CTB made of GP has the characteristics of quickly hardening and high strength. For full tailings, GP performance is superior to OPC.

(2) The hydration products of GP mainly include ettringite and C-S-H gel. As the curing age increases, the content of C-S-H gel increases, but the degree of crystallization does not increase significantly.

(3) The TG/DTG curves of the GP-CTB shows that it has three weight loss stages such as C-S-H gel dehydration, $CaCO_3$ decomposition, and some unknown hydration product decomposition during the experiment. While OPC-CTB has a weight loss stage of $Ca(OH)_2$ dehydration in addition to the above three weight loss stages.

(4) There is a good linear correlation between the UCS of GP-CTB and weight loss of the hydrated product C-S-H gel, and the relationship between the UCS of the CTB and the weight loss of C-S-H gel at different mass concentrations was established by using the one-way regression analysis method. While for the OPC-CTB, the UCS is related to the weight losses of C-S-H gel and $Ca(OH)_2$. And the relationship model between the UCS of the CTB

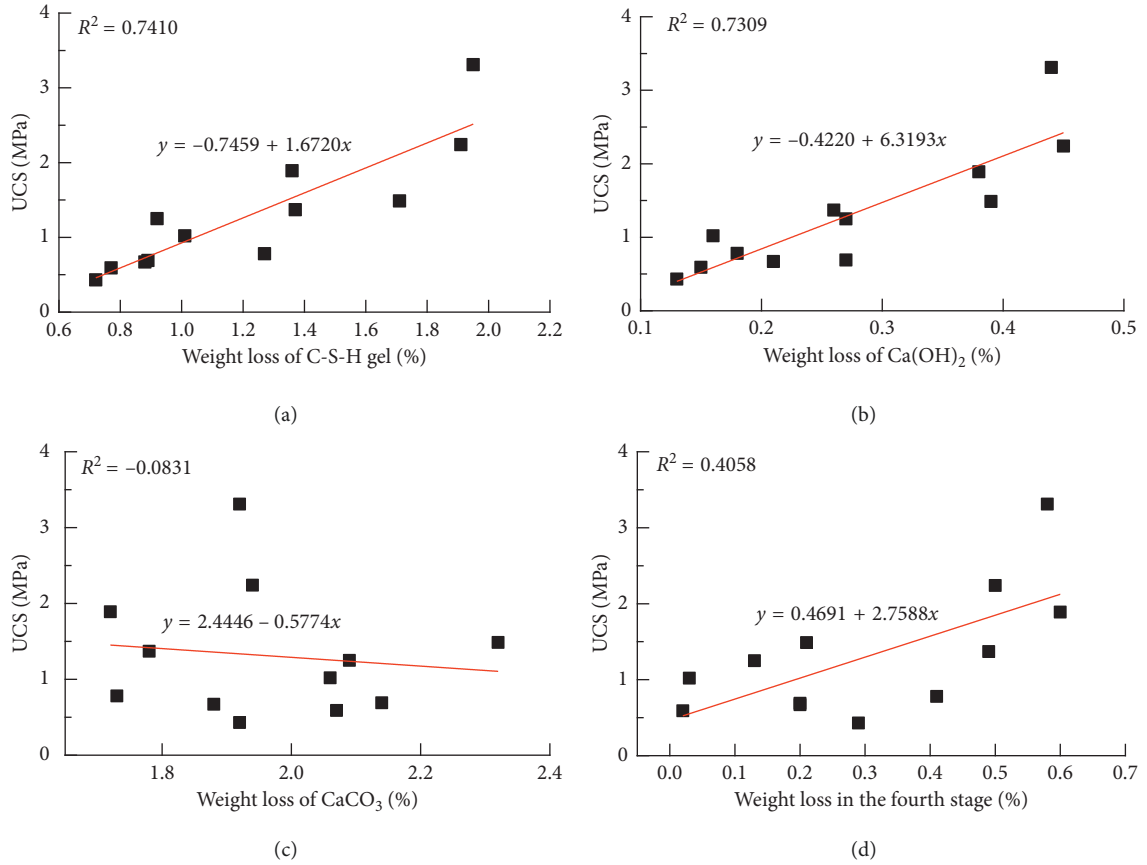

Figure 11: Fitting diagrams of weight losses of hydration products and strength of OPC-CTB (mass concentration 70%): (a) fitting diagram of weight loss of C-S-H gel and UCS of OPC-CTB; (b) fitting diagram of weight loss of $Ca(OH)_2$ and UCS of OPC-CTB; (c) fitting diagram of weight loss of $CaCO_3$ and UCS of OPC-CTB; (d) fitting diagram of weight loss in the fourth stage and UCS of OPC-CTB.

Table 4: Relationship model of strength and weight losses of hydration products.

Type of CTB	Concentration (%)	The model equation	R^2
GP-CTB	65	$R_c = 0.0256 + 1.8251x_1$	0.8749
	68	$R_c = -0.3204 + 2.3223x_1$	0.7867
	70	$R_c = -0.2756 + 2.4557x_1$	0.9087
	72	$R_c = 0.3006 + 2.6276x_1$	0.8008
	75	$R_c = -1.1966 + 4.7837x_1$	0.7415
	78	$R_c = 0.8783 + 5.0632x_1$	0.7046
OPC-CTB	65	$R_c = -1.0637 + 0.9820x_1 + 2.7345x_2$	0.7834
	68	$R_c = -1.9223 + 1.8580x_1 + 2.0974x_2$	0.8040
	70	$R_c = -0.7184 + 0.9294x_1 + 3.2307x_2$	0.7692
	72	$R_c = -2.5127 + 2.4890x_1 + 3.1285x_2$	0.8084
	75	$R_c = -4.1528 + 3.9300x_1 + 5.3372x_2$	0.8343
	78	$R_c = -3.2128 + 2.8356x_1 + 6.7251x_2$	0.8319

R_c is the UCS of CTB, MPa; x_1 is the weight loss of C-S-H gel, %; x_2 is the weight loss of $Ca(OH)_2$, %; R^2 is the correlation coefficient.

and the weight losses of the two hydrated products is established through the binary linear regression analysis.

This paper studied the relationship model between the UCS of the CTB and the weight loss of the hydrated product, and it also provides ideas and methods for analysis of hydration products by thermal analysis and interpretation of the strength changes of cement-based materials. However, there are still some shortcomings, for example, we do not know about the hydrated product decomposed in the temperature range of 1100~1200°C. It should be further studied in the future.

Data Availability

The data used to support the findings of this study are available from the corresponding author upon request.

Conflicts of Interest

The authors declare no conflicts of interest.

Acknowledgments

This work was supported by the National Key Research and Development Project (Project no: 2018YFC0808400), "Research on Safety, Technology, and Equipment Development for Metal Mines in High-Altitude and Alpine Regions."

References

[1] W. Sha, E. A. O'Neill, and Z. Guo, "Differential scanning calorimetry study of ordinary Portland cement," *Cement and Concrete Research*, vol. 29, no. 9, pp. 1487–1489, 1999.

[2] M. Fall and M. Pokharel, "Coupled effects of sulphate and temperature on the strength development of cemented tailings backfills: Portland cement-paste backfill," *Cement and Concrete Composites*, vol. 32, no. 10, pp. 819–828, 2010.

[3] J. W. Bullard, H. M. Jennings, R. A. Livingston et al., "Mechanisms of cement hydration," *Cement and Concrete Research*, vol. 41, no. 12, pp. 1208–1223, 2011.

[4] W. Xu, P. Cao, and M. Tian, "Strength development and microstructure evolution of cemented tailings backfill containing different binder types and contents," *Minerals*, vol. 8, no. 4, p. 167, 2018.

[5] Z. Shui, T. Sun, Z. Fu, and G. Wang, "Dominant factors on the early hydration of metakaolin-cement paste," *Journal of Wuhan University of Technology-Mater. Sci. Ed.,* vol. 25, no. 5, pp. 849–852, 2010.

[6] K. Mori, T. Fukunaga, M. Sugiyama, K. Iwase, K. Oishi, and O. Yamamuro, "Hydration properties and compressive strength development of low heat cement," *Journal of Physics and Chemistry of Solids*, vol. 73, no. 11, pp. 1274–1277, 2012.

[7] K. Sisomphon and L. Franke, "Evaluation of calcium hydroxide contents in pozzolanic cement pastes by a chemical extraction method," *Construction and Building Materials*, vol. 25, no. 1, pp. 190–194, 2011.

[8] E. Knapen and D. van Gemert, "Cement hydration and microstructure formation in the presence of water-soluble polymers," *Cement and Concrete Research*, vol. 39, no. 1, pp. 6–13, 2009.

[9] Z. H. Ou, B. G. Ma, and S. W. Jian, "Comparison of FT-IR, thermal analysis and XRD for determination of products of cement hydration," *Advanced Materials Research*, vol. 168-170, pp. 518–522, 2010.

[10] L. Kun, A. B. Chen, X. J. Shang et al., "The impact of mechanical grinding on calcium aluminate cement hydration at 30°C," *Ceramics International*, vol. 45, no. 11, pp. 14121–14125, 2019.

[11] Y. Feng, J. Kero, Q. Yang et al., "Mechanical activation of granulated copper slag and its influence on hydration heat and compressive strength of blended cement," *Materials*, vol. 12, no. 5, p. 772, 2019.

[12] M. Fall, J. C. Célestin, M. Pokharel, and M. Touré, "A contribution to understanding the effects of curing temperature on the mechanical properties of mine cemented tailings backfill," *Engineering Geology*, vol. 114, no. 3-4, pp. 397–413, 2010.

[13] H. Q. Jiang, M. Fall, and C. Liang, "Yield stress of cemented paste backfill in sub-zero environments: experimental results," *Minerals Engineering*, vol. 92, pp. 141–150, 2016.

[14] F. Kun and M. Fall, "Effects of curing temperature on shear behaviour of cemented paste backfill-rock interface," *International Journal of Rock Mechanics and Mining Sciences*, vol. 112, pp. 184–192, 2018.

[15] Y. J. Wang, L. Cheng, D. X. Li, and X. Q. Wu, "Advantages and complementary effects of slag fly ash," *Journal of Nanjing University of Chemical Technology*, vol. 22, no. 2, pp. 26–30, 2000.

[16] Y. Hou, P. Ding, D. Han, X. Zhang, and S. Cao, "Study on the preparation and hydration properties of a new cementitious material for tailings discharge," *Processes*, vol. 7, no. 1, p. 47, 2019.

[17] S. Ding, "Research on the relationship between microstructure and macroscopic performance of shotcrete," Master thesis, Xi'an University of Architecture and Technology, Xi'an, China, 2014.

[18] M. Singh and M. Garg, "Activation of gypsum anhydrite-slag mixtures," *Cement and Concrete Research*, vol. 25, no. 2, pp. 332–338, 1995.

[19] B. Lothenbach, F. Winnefeld, C. Alder, E. Wieland, and P. Lunk, "Effect of temperature on the pore solution, microstructure and hydration products of Portland cement pastes," *Cement and Concrete Research*, vol. 37, no. 4, pp. 483–491, 2007.

[20] M. Pokharel and M. Fall, "Combined influence of sulphate and temperature on the saturated hydraulic conductivity of hardened cemented paste backfill," *Cement and Concrete Composites*, vol. 38, pp. 21–28, 2013.

[21] G. Z. Jiang, A. X. Wu, H. Li, Y. M. Wang, and H. J. Wang, "Long-term strength performance of sulfur tailings filling and its affecting factors," *Journal of Central South University*, vol. 49, no. 6, pp. 1504–1510, 2018.

[22] X. F. He, "Non-iso thermal decomposition kinetics and theoretical study of cement hydration products," Doctor dissertation, Southeast University, Nanjing, China, 2016.

[23] X. Yang, J. Wang, D. Hou, C. Zhu, and M. He, "Effect of dry-wet cycling on the mechanical properties of rocks: a laboratory-scale experimental study," *Processes*, vol. 6, no. 10, p. 199, 2018.

[24] B. W. Wang and C. L. Wang, *Management of Metal Mine Goafs and Safety Recovery of Residual Resources*, Metallurgical Industry Press, Beijing, China, 1st edition, 2019.

[25] A. Rayed, B. Omrane, A. K. Mohamed, M. M. Abdeliazim, and S. Chokri, "Study of the effects of marble powder amount on the self-compacting concretes properties by microstructure analysis on cement-marble powder pastes," *Advances in Civil Engineering*, vol. 2018, Article ID 6018613, 13 pages, 2018.

[26] Z. S. Lin, *Cementitious Materials Science*, Wuhan University of Technology Press, Wuhan, China, 1st edition, 2014.

[27] Y. Xiao, X. Y. Zhang, X. L. Shi et al., "X-ray diffraction analysis of calcium silicate hydration process," *Journal of Yili Normal University (Natural Science Edition)*, vol. 9, no. 1, pp. 38–40, 2015.

[28] Q. F. Li, "Effect of inorganic salt admixtures on microstructure of hydrated C3S and C3A in cement," Doctor dissertation, Harbin Institute of Technology, Harbin, China, 2016.

[29] W. C. Li, "Characteristics and mechanism of sulphate effecton the early age properties of cemented paste backfill," Doctor dissertation, China University of Mining and Technology (Beijing), Beijing, China, 2016.

[30] L. Alarcon-Ruiz, G. Platret, E. Massieu, and A. Ehrlacher, "The use of thermal analysis in assessing the effect of temperature on a

cement paste," *Cement and Concrete Research*, vol. 35, no. 3, pp. 609–613, 2005.

[31] P. L. Esteves, "On the hydration of water-entrained cement–silica systems: combined SEM, XRD and thermal analysis in cement pastes," *Thermochimica Acta*, vol. 518, no. 1-2, pp. 27–35, 2011.

[32] I. Pane and W. Hansen, "Investigation of blended cement hydration by isothermal calorimetry and thermal analysis," *Cement and Concrete Research*, vol. 35, no. 6, pp. 1155–1164, 2005.

[33] W. Li and M. Fall, "Strength and self-desiccation of slag-cemented paste backfill at early ages: link to initial sulphate concentration," *Cement and Concrete Composites*, vol. 89, pp. 160–168, 2018.

[34] L. Yu, *Micro- Properties of Cement Concrete*, China Building Industry Press, Beijing, China, 1st edition, 2017.

[35] N. R. Yang and W. H. Yue, *Handbook of Inorganic Matalicid Materials Atlas*, Wuhan University of Technology Press, Wuhan, China, 1st edition, 2000.